Performance Analysis of Photovoltaic Passive Heat Storage System with Microencapsulated Paraffin Wax for Thermoelectric Generation

Mohamed Nazer[1]*, Muhammad Fadzrul Hafidz Rostam[2], Se Yong A/L Eh Noum[1], Mohammad Taghi Hajibeigy[1], Kamyar Shameli[3]

School of Computer Science and Engineering Taylors University, Jalan Taylors, 47500 Subang Jaya, Selangor, Malaysia [1]

Jeffrey Sachs Center on Sustainable Development, Sunway University, Jalan Universiti, Bandar Sunway, 47500 Petaling Jaya, Selangor, Malaysia [2]

Malaysia-Japan International Institute of Technology, Universiti Teknologi Malaysia, Jalan Sultan Yahya Petra, 54100 Kuala Lumpur, Malaysia [3]

* Correspondence: nazer@outlook.my Tel: 0107126670

https://doi.org/10.37934/jrnn.1.1.7590

ABSTRACT

The depletion of non-renewable energy sources and negative effects towards the environment push research towards the widespread adoption of renewable energy sources such as solar energy. The main drawback of solar panels is that temperatures above 27°C will result in an efficiency drop of 0.1-0.5%/°C. In previous studies, usage of photovoltaic thermal (PVT) systems was mainly for the purpose of heating water, warming buildings, and drying crops. This research will focus on the usage of a standalone PVT and thermoelectric generator (TEG) system whereby it uses heat extracted from the PVT system for thermoelectric generation. A passive standalone PVT-TEG system design with microencapsulated paraffin wax as a phase change material (PCM) as a heat storage medium was created. The heat stored in the PCM is used as a heat source for thermoelectric generation. To extract the heat from the PV panel, an aluminum heatsink underneath the PV panel is used as a heat absorber to passively extract heat without external power sources. This setup reduces the surface temperature by 22.7°C. Transient thermal analysis and thermoelectric simulation of the system was conducted through Computational Fluid Dynamics (CFD) using ANSYS 2019 software. The error recorded between the experimental and simulation results was 4.2%. This proposed system panel successfully increased the electrical efficiency of the PV panel by approximately 12.8%, where the overall electrical power produced shows a significant increase from 7.7W to 17.7W.

Keywords:

Renewable energy, PVT system, TEG, CFD simulation, Transient thermal analysis, Microencapsulated paraffin wax

Penerbit
Akademia Baru

1. Introduction

With the push towards research into renewable energy, solar energy in particular has been widely studied and researched as it has one of the highest potentials to be used as an energy source in multiple functions. This has resulted in the development of photovoltaic (PV) panels which harness sunlight to be converted into energy. Currently, the main drawback of photovoltaic energy is its efficiency. Current commercially available PV panels have an efficiency of approximately 24%, and the efficiency of the panel further degrades during its operation. The efficiency loss of PV panels during its operation can be divided into two: electrical loss, which is related to the material of the PV panel, and optical loss, which can be further divided into 3 sections: shadow, reflection and unabsorbed radiation [1]. This paper will focus on energy loss due to unabsorbed radiation. The unabsorbed radiation on the PV panel is converted to heat. When the PV panel temperature increases above 27°C, the efficiency of the PV panel drops by 0.1% to 0.5% per 1°C increment in temperature [2].

There are two ways to improve the efficiency of the PV panel from unabsorbed radiation. The first method is to extract the excessive heat from the PV panel using water or air. Extracting heat from the PV panel lowers the operating temperature of the panel, which helps to increase the efficiency of the PV panel. This type of system is called a photovoltaic thermal (PVT) system. Secondly, the excessive heat from the PV panel is converted to electricity using thermo-electric process. This type of system is called a photovoltaic thermoelectric generator system (PVT-TEG).

A PVT system comprises of several components: a PV panel, channel for cooling, and coolant (air/water). The heat stored in a PVT system is used to dry out agricultural production, keeping a room warm, and in water heaters [3]. Researchers have classified PVT systems into 2 different cooling systems: passive cooling (natural) and active cooling (forced) [4]. The easiest and most cost-effective cooling system is passive airflow, but it is less efficient in regions where the ambient temperature reaches 20°C or greater [5]. A PVT system consists of three different types, namely: PVT-air system, PVT-water system, and PVT-hybrid system. The PVT-hybrid system selected for this study is the PVT-TEG system [6]. A thermoelectric generator (TEG) is a solid-state device which converts thermal energy into electrical energy in a process called the Seebeck effect. In order for the Seebeck effect to occur, there must be a temperature gradient between both the hot and cold sides of the TEG [7]. Similar to PVT system PVT-TEG systems are classified into two sub-systems, which are: active and passive systems.

An active PVT-TEG system requires additional power to extract heat, such as from a heat exchanger. An study was conducted by Wu et al. [8] which analyzed the performance of a PVT-TEG system with a glazed PV panel and nanofluid as coolant. The results from the analysis show that glazed PV panel (11% efficiency) performed slightly better compared to unglazed PV panel (10.6% efficiency). The use nanofluid as coolant helps to increase the efficiency by 0.28% and 0.48% for unglazed and glazed PV panel respectively. Kilkis [9] proposed a multi-layered composite PVT module which consists of several small PVT cartridges, each fitted with PV cells, TEG modules, PCM layer, and a flat plate solar collector. Pilot scale tests have shown that the total power generation efficiency of this system is improved by up to 30% with the TEG. Combined usage of cobalt oxide (Co_3O_4) nanofluid and a paraffin wax phase change material as a cooling method on the performance of a PVT-TEG system was studied by Rajaee et al. [10]. The study concluded that by using both the PCM and 1% of Co_3O_4 nanofluid, the overall electrical efficiency of the system was improved by 12.28% compared to the water-cooling method. In addition, a simulation was conducted by Kolahan et al. [11] on a PVT-TEG system with aluminum oxide (Al_2O_3) nanofluid used as the working fluid, as it is found to improve the working performance of the system. From the simulation, it is shown

that the combined PVT-TEG system with nanofluid has an improved overall electrical efficiency of 2.5%-4% over the base PVT system. Research by Soltani et al. [12] was conducted an indoor experiment to test the efficacy of a PVT-TEG system with several different types of coolants, which were water, air, and two types of nanofluids: silicon dioxide (SiO_2-water), and iron oxide (Fe_3O_4-water). Energy, exergy, and environmental analysis was done with each coolant to investigate its performance on the PVT-TEG system. Based on the results from each setup, the setup with the SiO_2-water as a nanofluid provided the maximum exergy efficiency at a fixed rate of irradiation of 900W/m², thus indicating that the usage of nanofluids as a coolant will increase exergy efficiency. Despite the advantages of active PVT-TEG systems, the drawback with active systems lies in the difficulty of large-scale solar implementation. This is due to the high-power demand for active heat extraction methods and its complexity due to the high number of additional components for heat extraction.

In contrast, passive PVT-TEG systems rely on natural cooling to extract heat to power the TEG in the system. Performance analysis of a thermal interface material on a PVT-TEG system was done by Zhang et al. [13], and found that the power generated by the PV cells increased by at least 14%, whereas the power generated by the TEG had at least a 60% increase due to the lower thermal contact resistance. Analysis was done by Adham et al. [14] on the performance on PV-TEG system using heat pipe using nemerical method. The heat from the PV panel is extracted using a copper heatpipe. From the analysis, it was concluded that as the irradiance increases, the PV panel efficiency also increases, as more solar energy is available at the collector per unit area for electricity generation, in addition to increased TEG conversion efficiency as higher radiation permits higher temperature difference across the TEG module plate. Bjork and Nielsen [15] pointed out that the degradation of PV performance with temperature is shown to dominate the increase in power produced by the TEG due to the low efficiency of the TEG. For c-Si, CIGS and CdTe PV cells the combined system produces a lower power and has a lower efficiency than the PV alone, whereas for an a-Si cell the total system performance may be slightly increased by the TEG. An experiment on PVT-TEG was done by Dallan et al. [16] which analyzed the viability of series connected TEG to the PV panel. The results show that the power output of PV-TEG is 39% higher compared to PV panel alone. The theoretical performance of a hybrid PVT-TEG system with multi-crystalline silicone was analyzed by Challa et at. [17]. At the end of the research, it was concluded that the overall efficiency of the system is 6% higher compared to standalone PV. Research conducted by Du et al. [18] analyzed the performance of the PVT-TEG system combined with PCM. The results from the experiment shows that with the help of the PCM, the electrical efficiency of the system increased by 9.5%. A comparison was made between the performance of a hybrid PVT-TEG system with a conventional one by Li et al. [19] on a summer day in China, where results show that the hybrid system has an efficiency higher than 14.3%, and having a higher electrical output than a conventional system. An experiment was conducted by Xuan and Zhang [20] which replaced the flat structure on the conventional PVT-TEG system to a V-type shaped structure. Experiments show that the V-shape groove is proven to be a superior method to increase the absorption of solar energy which will lead to an increase in the efficiency of the PVT-TEG system by 20%. For passive PVT-TEG systems most authors used TEG as a thermal absorber by placing the TEG directly underneath the PV panel or used a solar concentrator to increase the surface temperature of the PV and TEG which will increase the degradation of both the PV panel and TEG. Most of the thermal recovery from previous research is mainly used to lower the operating temperature of the PV panel and water heater.

This research aims to design a passive PVT system for thermoelectric generation which will help to lower the operating temperature of the PV panel. Heat is extracted by using an aluminum heatsink which acts as a heat absorber, where it is stored in a PCM. The heat stored in the PCM is then

redistributed to the TEG which produces electricity. This will help to increase the electrical efficiency of the system.

2. Research Methodology

This research is divided into 4 sections. An indoor experiment is first conducted to determine the temperature of each layers in the PVT system. Using the data from the experiment, a thermal analysis of the PVT system was conducted using ANSYS transient thermal analysis, followed by an error analysis between the experiment and the simulation is done to validate the experiment. Using the data from the simulation, a transient thermal analysis of a single TEG is conducted to determine the temperature gradient between the hot and cold sides of the TEG module. The temperature gradient of the TEG module is then used to predict the output power of the TEG module. At the end of the research, by using the experimental data and the simulation data, the overall output power and efficiency of the PVT-TEG can then be determined. The flowchart to compute the overall efficiency is illustrated in Figure 1.
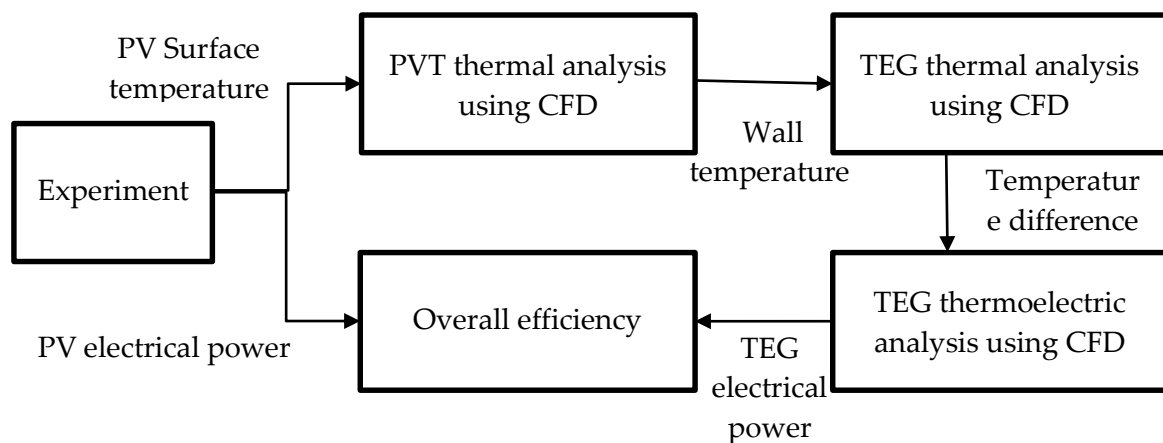
Figure 1. Flowchart of computing the overall efficiency of the system using data from experiment and simulation

### 2.1. Design of proposed photovoltaic-thermoelectric generator system

The objective of this research is to analyze the thermal efficiency of the proposed PVT system using Computational Fluid Dynamics (CFD). Figure 2 illustrates the exploded view of the internal components. The proposed designed consists of 7 different components layered on top of one another. The PV panel consists of 4 different layers which are glass, ethylene vinyl acetate (EVA), silicon cell and tedlar. However, in this simulation, the PV panel is only considered as a single layer of glass in order to simplify the computational time. The heat from the PV panel is extracted from an aluminum heatsink which is submerged into water. Water is used to evenly distribute heat around the PCM. The PCM will slowly heat up the aluminum container of the TEG and the cold side of the TEG produces thermoelectricity when there is no adequate amount of sunlight to produce electricity from the PV panel. The main drawback of PCM is its low thermal conductivity, to overcome this issue microencapsulated PCM was used in this research to enhance the thermal conductivity of the PCM The proposed design consists of 70 TEGs which are connected in series around the container.
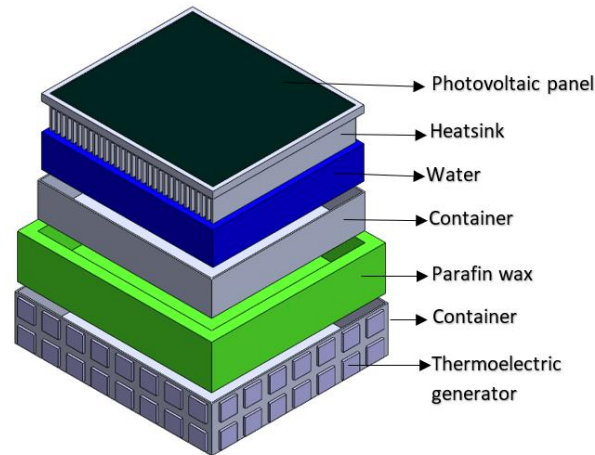
Figure 2. Exploded view of the proposed design.

2.2. Geometric modelling and thermal properties of PVT system

The PVT system and the TEG was modelled separately to reduce complexity of the simulation. A 2D model of the PVT system and TEG was drawn using SolidWorks 2019. A TEG consists of 8 rows on p-n junctions connected in series. As the model was drawn in 2D, only one row of p-n junction was analyzed. The resulting geometry is presented in Figure 3. The design uses a glazed PV panel, therefore it was assumed that the PV layer is to be made from glass. In the simulation, it was assumed that there is no air gap between each layer. The thermal properties of the PVT system is listed in Table 1.
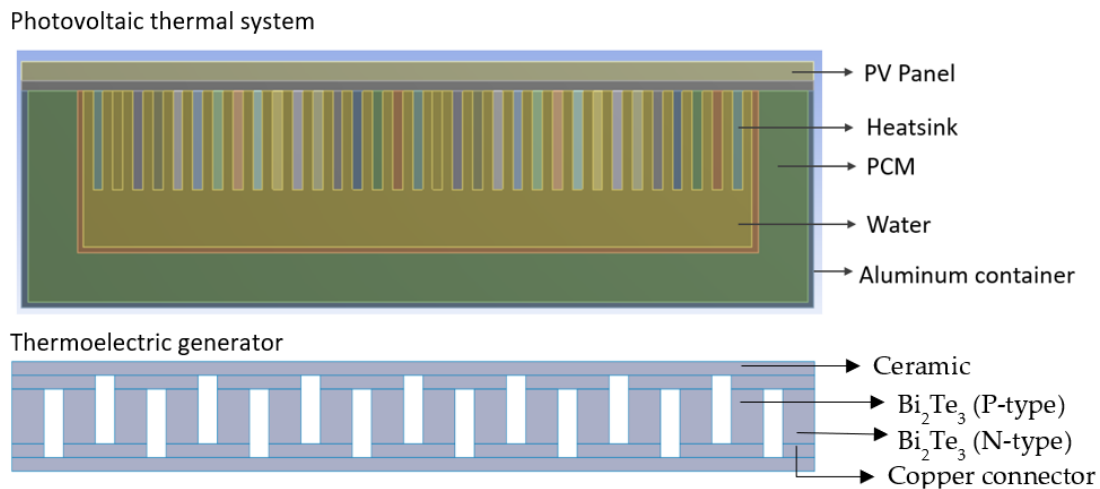

Figure 3. 2-Dimensional view of the proposed system.

Table 1. Thermal properties of PVT system.

Layers	Thermal conductivity W/m°C	Specific heat capacity J/kg°C	Density Kg/m³	Seebeck coefficient (V/K)
Glass (PV)	1.8	500	3000	-
Aluminium	204	996	2707	-
Water	0.6	4200	1000	-
Bi_2Te_3	1.6	154.4	7740	$\pm 200 \times 10^{-6}$

Copper	350	385	8920	6.5×10^{-6}
Phase change material				
Microencapsulated PCM		Paraffin wax		
Viscosity (Kg/ms) @ 50% microcapsule		1.9		
Density (Kg/m^3)		900		
Thermal conductivity (W/m$^{\circ}$C) @ 50% microcapsule content.		0.35		
Specify heat capacity (J/kg$^{\circ}$C) @ 50% microcapsule content.		2900		
Melting point ($^{\circ}$C)		25		

2.3. Meshing methods for simulation

A mesh test was performed with four different methods of meshing, which are: quadrilateral meshing, quadrilateral refinement meshing at contact region, triangular meshing, and triangular refinement meshing at contact region, with different mesh sizes ranging from 1mm to 10mm. The refinement was conducted at each contact area between each layer, this helps to increase the accuracy of the of the computational value when the heat is transferred from one layer to another. Based on the different mesh sizes, its effect on the temperature of the PCM is observed and compared with experimented data. The different method used during the mesh is illustrated in Figure 4.
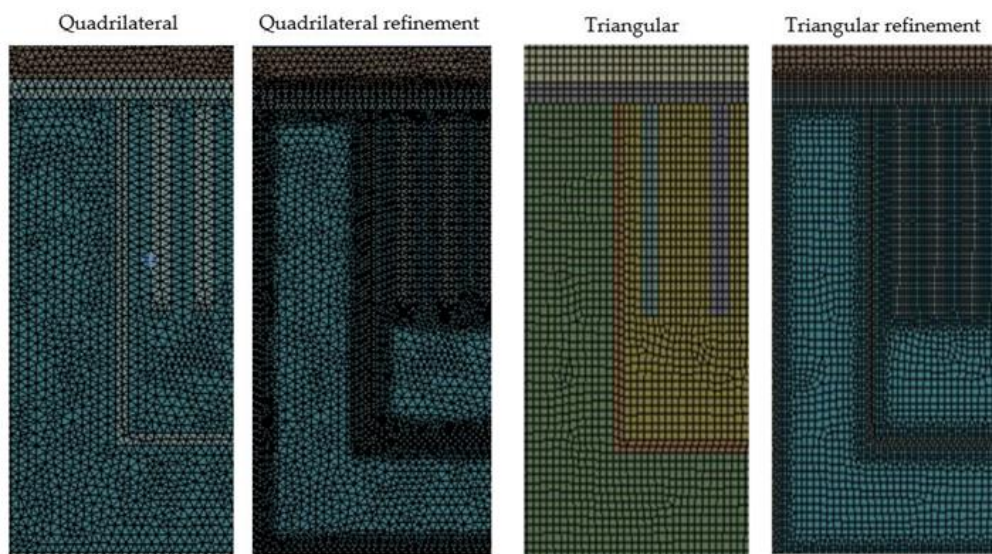
Figure 4. Type of mesh used for simulation

2.4. Boundary condition of photovoltaic thermal system

The simulation was divided into 3 parts to reduce the computational time, which are: transient thermal analysis of the PVT to predict the thermal performance of PVT, transient thermal analysis of the TEG to predict the thermal performance of TEG, and steady state thermoelectric analysis of the TEG to predict the thermoelectric performance of the TEG.

Apart from that, it was assumed that the heat transfer through each layer only occurs through conduction whereas heat loss through radiation is ignored. As for convection, the simulation was

conducted in a controlled environment with the wind velocity at 0 m/s and the outer layer of the PVT system is covered by the TEG, therefore it was assumed that there is no energy loss due to convection.

2.5. Boundary condition of thermoelectric generator

The TEG is simulated in an outdoor environment condition as there is no wind in an indoor environment condition, therefore heat loss due to convection is assumed to be 0m/s. Without convection, the temperature difference between the hot and cold sides of the TEG is very small, thus the TEG is simulated in an outdoor environment where the average wind velocity in Malaysia is approximately 3 m/s [21]. The convective heat transfer of air for 3m/s is approximately 20 W/m²K. The heat transfer coefficient is applied to the cold side of the TEG [22]. The temperature of the hot side of the TEG is from the outer wall temperature from the PVT thermal analysis which was previously discussed.

The thermoelectric simulation was conducted on a steady state thermal analysis, therefore the temperature on the hot and cold sides are kept constant. The temperature difference between both sides gradually increases from 20°C to 100°C, following the temperature difference given by the manufacturer. To measure the output current from the TEG, the potential difference between the P-type and N-type legs is kept at 0V. To measure the voltage, only the P-type leg is kept at 0V, this will enable us to measure the potential difference between the p-type and n-type legs.
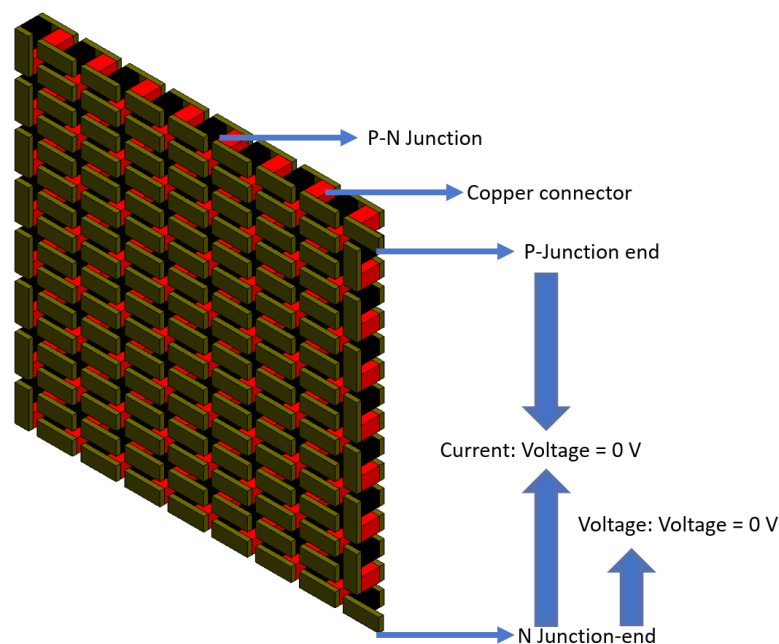
Figure 5. Boundary condition for thermoelectric generation

2.6. Experimental setup

The primary objective of this experiment is to evaluate the electrical and thermal performance of the proposed PVT system. For this experiment, the thermal performance of the organic PCM was analyzed. Microencapsulated organic paraffin with a melting temperature of 25°C was used as the PCM in this experiment.

The system is evaluated in an indoor controlled environment with parameters such as ambient temperature, irradiance, and wind speed being kept constant in the experiments. The ambient temperature is set to room temperature at 24°C. The irradiance from the artificial light source is kept

constant at approximately 800 W/m². Wind speed is set to 0 m/s. A rheostat with a resistance of 33Ω is used as a load for the PV panel. The temperature of each layer is set at room temperature at the beginning of the experiment.

As mentioned above, the PVT system is divided into four different layers: the PV panel, aluminum heatsink, water, and PCM. The PVT system consists of a glazed flat plate polycrystalline silicon solar panel, and a heatsink was attached under the PV panels to extract excess heat from the PV panel as well as to improve the thermal performance of the system. The heatsink is submerged under the water to distribute the heat around the PCM evenly. The setup for the experiment is shown in Figure 6. A pyranometer was used to record the irradiance of light, and a thermocouple was used to record the temperature of each layer of the PVT system.
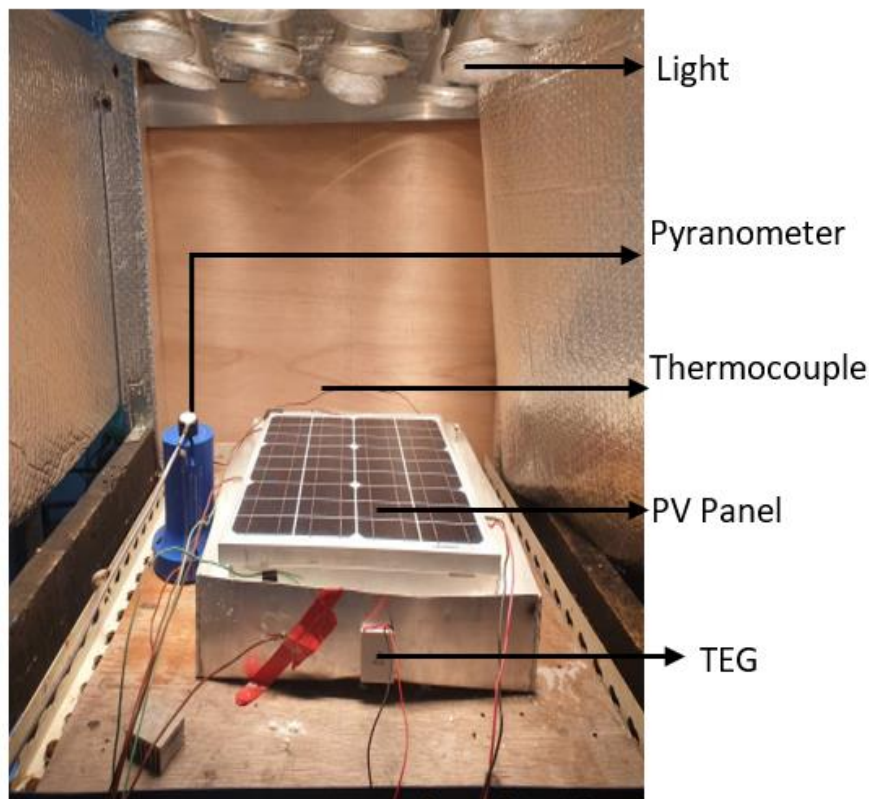

Figure 6. Experimental setup

3. Results and Discussion

The experiment was conducted to measure the surface temperature of the PV module and the effects of different heat removal elements from the PV module under various conditions in a controlled environment. The surface temperature of the PV panel was recorded every second for a period of 1 hour. The irradiance from the artificial light was set at approximately 800W/m² and the room temperature was kept constant at 27°C.

The temperature of the surface of the PV panel was recorded using a data logger at every second. Results from the experiment is shown in Figure 7, where it can be seen that the temperature of the PV panel increases to 70°C when it is exposed to 800 W/m² irradiance. Thus, an assumption is made for the simulation where the surface temperature of the PV panel was kept at a temperature of 70°C for 1 hour.
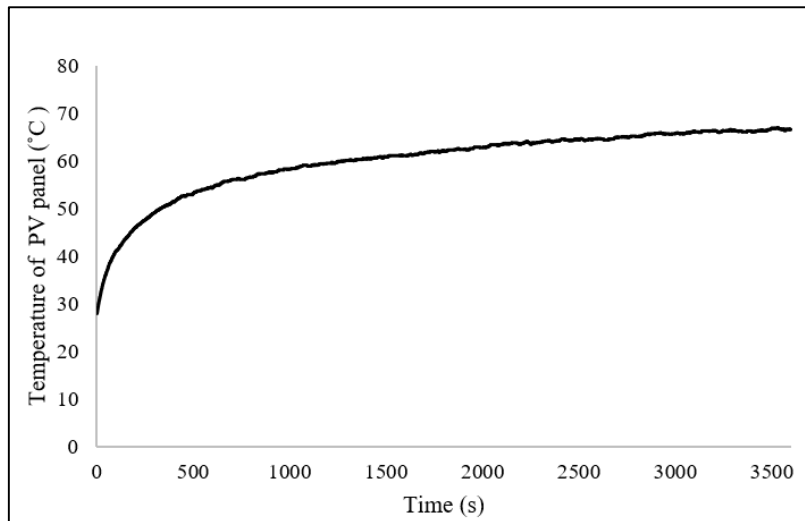
Figure 7. Surface temperature of photovoltaic panel when exposed to irradiance of 800W/m2 for one hour

3.1 Relationship between PV temperature and output power

A PV panel is similar to semiconductor devices in the sense that they are both sensitive to temperature. The increase or decrease in temperature affects the output power of the system. Figure 8 represents the relationship between the operating temperature and the output power of the PV panel. At the beginning of the experiment, the output power from the PV panel was 12.02W at 27 °C with an electrical efficiency of 12.3%. After exposing the PV panel to an irradiance of 800W/m² for 1 hour, the output power from the PV panel drops to 7.46W at 66.7°C with an electrical efficiency of 7.6%. This indicates a 4.7% drop in efficiency with a temperature increment of 39.7°C, thus showing an efficiency drop of 0.12% per 1°C increment.

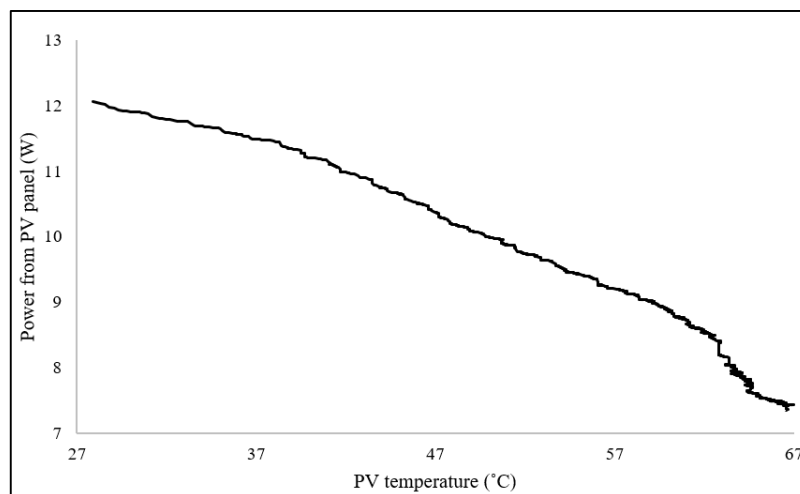$$\eta_{PV} = \frac{P_{PV}}{S \times A} \times 100 \tag{1}$$

Where:

P_{PV} = Output power from PV panel (W)

S = Irradiance (W/m²)

A = Area of PV panel (m²)

$$\eta_{PV} = \frac{12.02}{800 \times 0.14} \times 100$$
$$\eta_{PV} = 12.3\%$$

Figure 8. Output power of the photovoltaic panel VS temperature of the PV panel

83

The experiment was conducted in three different setups, which consisted of the PV panel alone, PV panel along with heatsink, and lastly PV panel with PCM. When the heatsink is submerged inside the water, the surface temperature of the PV panel reduces drastically. Table 2 summarizes the temperature of the PV panel after 1 hour. By looking at Figure 9, it can be seen that after 1 hour, the final temperature of the PV panel is 89.3 ˚C, and with the addition of the heatsink, the temperature of the PV panel drops to 76.7˚C and with water and PCM the temperature of the PV panel drops further to 66.7˚C. Therefore, by simply submerging the heatsink to the water the temperature of the PV panel drops by 22.6˚C, which will help to increase the electrical efficiency of the PV panel. This shows that the setup helps to cool down the PV panel by 22.6˚C, which gives an electrical improvement of 2.7% compared to PV panel alone.
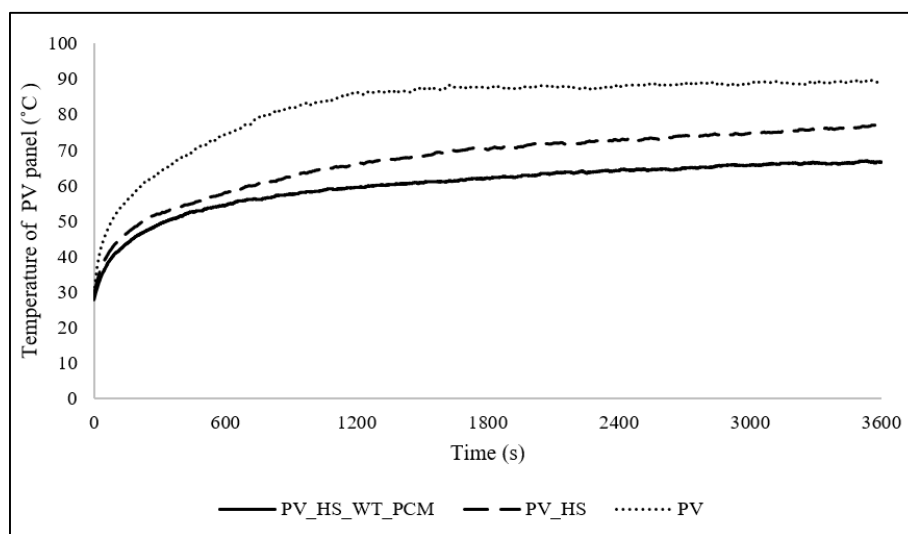
Figure 9. Surface temperature of the PV panel with different setup.

Table 2. Final temperature of PV after 1-hour indoor experiment.

Setup	Temperature of PV panel after 1 hour (˚C)
PV panel alone (PV)	89.3
PV panel with heatsink (PV_HS)	76.7
PV panel with heatsink, water, and PCM (PV_HS_WT_PCM)	66.6

3.2 Results from meshing test for the simulation

As previously mentioned, four different types of meshing was tested during the simulation. The results of the meshing from both the quadrilateral and triangular refinements were compared with the experimental value. The experimental temperature of the PCM was 58.7˚C. By comparing the two refinement methods, it is found that quadrilateral refinement gives the closest value to the experimental results at a mesh sizing of 4mm, and triangular refinement method similarly gives a value closest to the experimental value at 4mm mesh size, however, it has a higher number of elements. Therefore, in comparison, quadrilateral refinement is most suitable to be used as it requires less computational time due to the lower number of elements. The results from the meshing is shown in Table 3.

Table 3. Mesh test results for different mesh method and different mesh size.

| Size	Tri		Tri_ref		Quad		Quad_ref	
mm	Elements	Temp	Elements	Temp	Elements	Temp	Elements	Temp
10	1921	50.6	7564	52.5	1006	52.0	3891	`53.4
9	2234	51.1	8760	53.0	1146	52.4	4414	53.6
8	2422	53.2	9436	54.4	1200	53.6	4693	54.3
7	2865	52.3	11139	52.0	1470	52.7	5667	52.0
6	3532	53.9	13099	53.4	1791	54.1	6593	53.4
5	5760	52.6	19154	53.2	2343	53.8	7987	53.5
4	8891	54.1	29103	55.3	3936	54.2	12803	55.2
3	14091	53.4	41563	52.8	6688	53.5	20242	52.9
2	29341	52.6	79327	52.0	15400	52.7	42754	52.2

3.3 Errors analysis of simulation

An assumption was made during the simulation where it was assumed that the heat was only applied from the surface of the PV panel and the ambient speed was 0m/s. Apart from that, during the experiment, the temperature was recorded at a particular point in each layer, whereas in the simulation, only the average temperature of each layer was able to be computed. These assumptions resulted in errors in comparing the experimental and simulation results.

Figure 10 represents the PCM temperature trend between the experiment and simulation. From the figure, it can be seen that both the experimental and simulation results display a similar trend. At the end of the heating process the experimental PCM temperature was 58.7˚C and simulated PCM temperature was 56.0˚C. This gives an error of approximately 4.60%.

Error = (58.7 - 56)/56 x 100

Error = 4.60 %
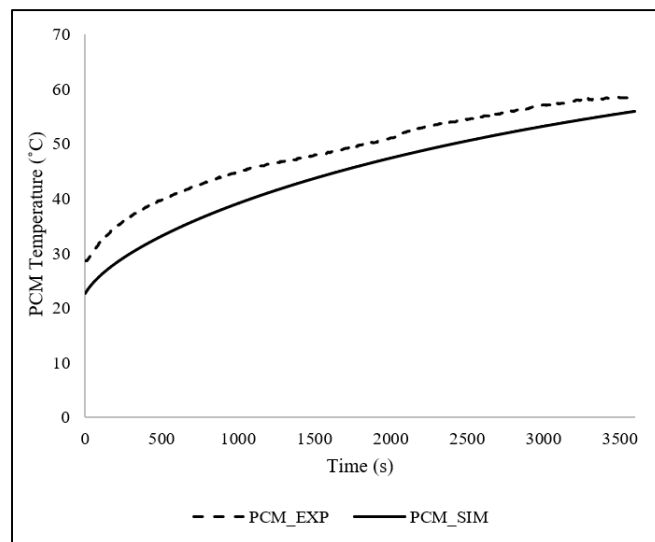
Figure 10. Experimental and simulation results of paraffin wax temperature

Table 4 shows the current from the simulation at different temperatures. Error analysis between the readings of the simulation and the data sheet can be determined by comparing the differences between the two readings. The error analysis can be calculated using the formula shown below:

$$Error_{Current} = \frac{I_{simulation} - I_{Actual}}{I_{Actual}} \text{ X } 100 \qquad (2)$$

For 20°C:

$Error_{Current} = \frac{233.6-225}{225} \times 100$

$Error_{Current} = 5.4\%$

$Error_{Voltage} = \frac{0.967-0.97}{0.97} \times 100$

$Error_{Voltage} = 0.28\%$

Table 4. Error analysis of thermoelectric generator.

	Current of 1 TEG			Voltage of 1 TEG		
Temp diff	I_Sim	I_Actual	I_Error	V_sim	V_Actual	V_Error
°C	mA	mA	%	V	V	%
20	212.9	225	5.37	0.967	0.97	0.28
40	425.0	368	15.48	1.935	1.8	7.48
60	636.1	469	35.63	2.902	2.4	20.91
80	846.4	558	51.69	3.869	3.6	7.48
100	1055.9	669	57.84	4.836	4.8	0.76

**I_Sim – Output current of the teg from simulation, V_Sim – Output voltage of the from simulation, I_Actual - Output current of the teg from datasheet, V_Actual - Output Voltage of the teg from datasheet

Figure 11 represents the simulation error with respect to the differences in temperature between the hot and cold sides of the TEG. Based on the figure, it is observed that an increase in temperature will result in an increase in the experimental error. In the simulation, the thermal conductivity is kept constant but in reality, the thermal conductivity of a specific material is highly dependent on several factors. These include the temperature gradient. Apart from that, thermal conductivity is proportional to electrical conductivity, therefore the error at higher temperature gradient is higher. Thermal conductivity has an insignificant effect on voltage therefore the error in voltage is low. Based on the figure, the observed error for temperatures below 20°C is less than 5.4% for current and 0.28% for voltage. In the simulation, it was observed that the temperature differences between the hot and cold sides did not exceed 20°C, thus, the error from the simulation is below 5.4% for current and 0.28% for voltage.
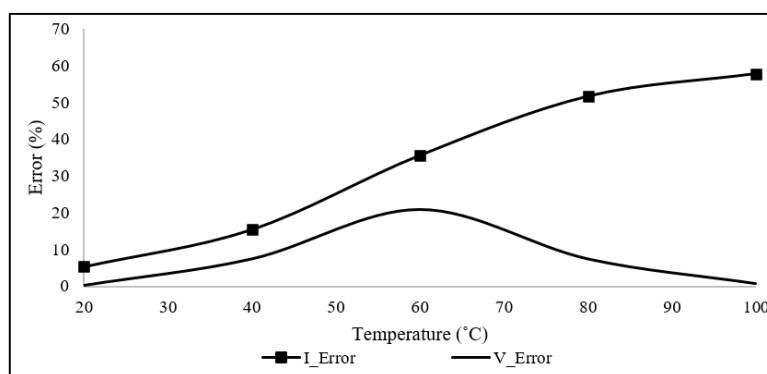

Figure 11. Error in the simulation Vs temperature of thermoelectric generator

3.4. TEG cooling

In order for better thermoelectric generation, the temperature difference between the hot and cold sides of the TEG has to be greater. The higher the temperature difference, the higher the thermoelectric generation. The performance of passive cooling with and without heatsink were tested

and compared during the simulation. It is observed that the setup of the TEG equipped with a heatsink has a higher temperature difference as compared to the setup with the TEG alone as shown in Figure 12.
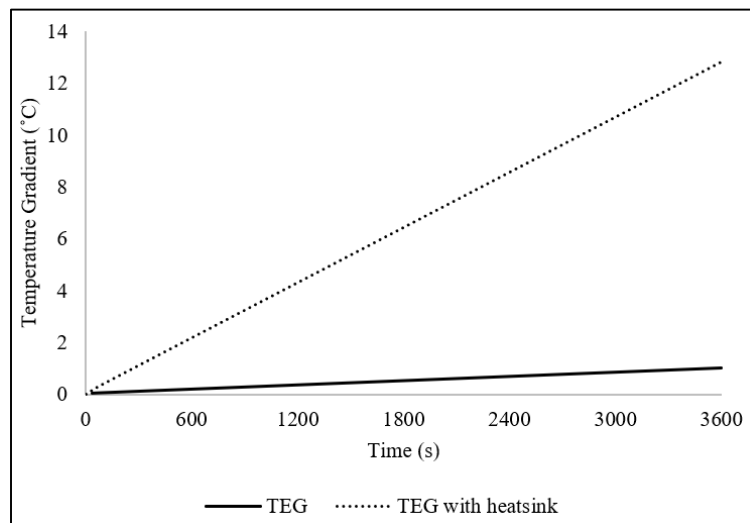
Figure 12. Temperature difference between TEG with and without heatsink

*3.5 Relationship between the thickness of the PCM and the temperature of the PCM*

The heat from the PV panel was extracted and stored in the PCM before being redistributed into the TEG. The amount of PCM determines the maximum temperature of heat which it can store. Figure 13 represents the relationship between the thickness and temperature of the PCM. From the graph, it can be seen that as the thickness of the PCM increases, the temperature of the PCM decreases. This is due to the increase in mass. When thickness is increased, more energy is required to increase the temperature as the mass is increased. Therefore, to store more heat, the thickness of the PCM should be smaller depending on the PCM melting temperature.
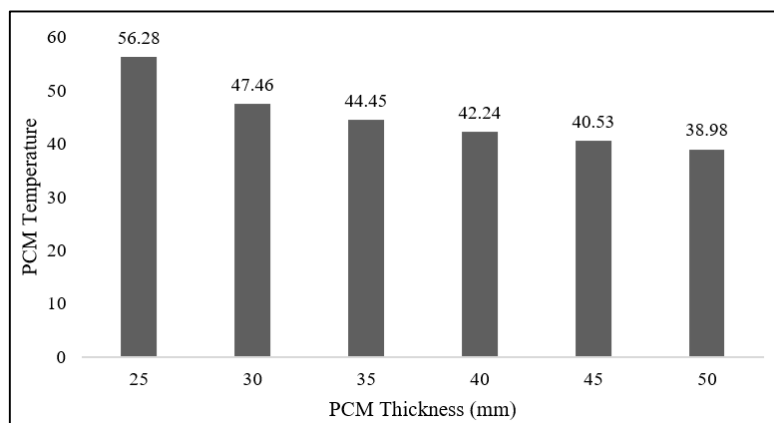
Figure 13. Relationship between PCM thickness and temperature of PCM

3.6 Electrical performance of the system

Figure 14 represents the output power of the system. The proposed design has 70 TEGs connected in series. From the figure, it can be seen that as time increases, the electrical power of the PV panel reduces whereas the electrical power of the TEG increases. This shows that excess heat from the PV panel is converted to thermoelectricity with the help of the TEG which results in a higher overall electrical output from the PVT system.
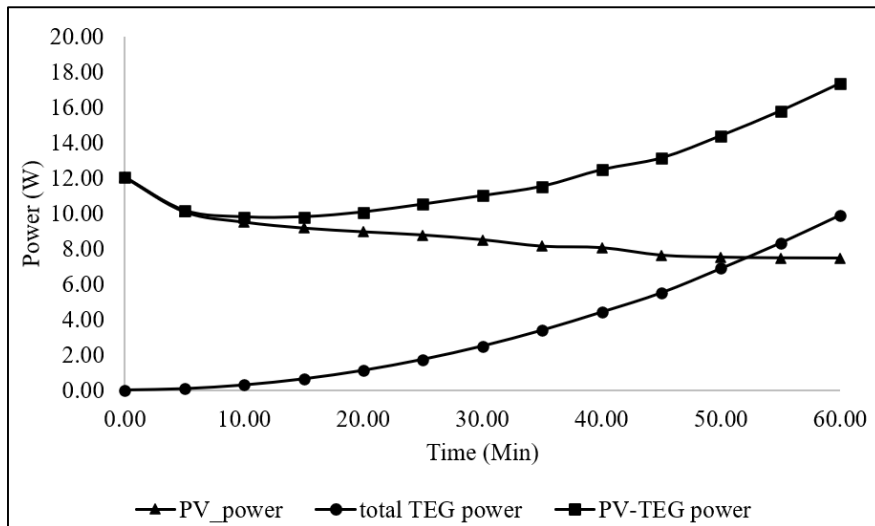
Figure 14. Electrical power of the system with and without thermoelectric generator

Figure 15 illustrates the electrical efficiency and the overall efficiency of the PV-TEG system. At the end of 1 hour, it can be seen that the electrical efficiency of the PV panel was 7.6%, indicating a drop of 4.7% compared to the initial electrical efficiency. With the use of the TEG, the overall electrical efficiency of the PV-TEG system after 1 hour increased to 17.7%, proving that the excess heat from the PV panel is converted to electricity with the help of the TEG. Thus, it can be concluded that the TEG system has an improvement of 10.1% compared to PV panel alone. The method to calculate overall efficiency is shown in equation 4.

$$\eta_{overall} = \frac{\text{Total electrical power from the system}}{S \, X \, A} \, X \, 100 \tag{4}$$
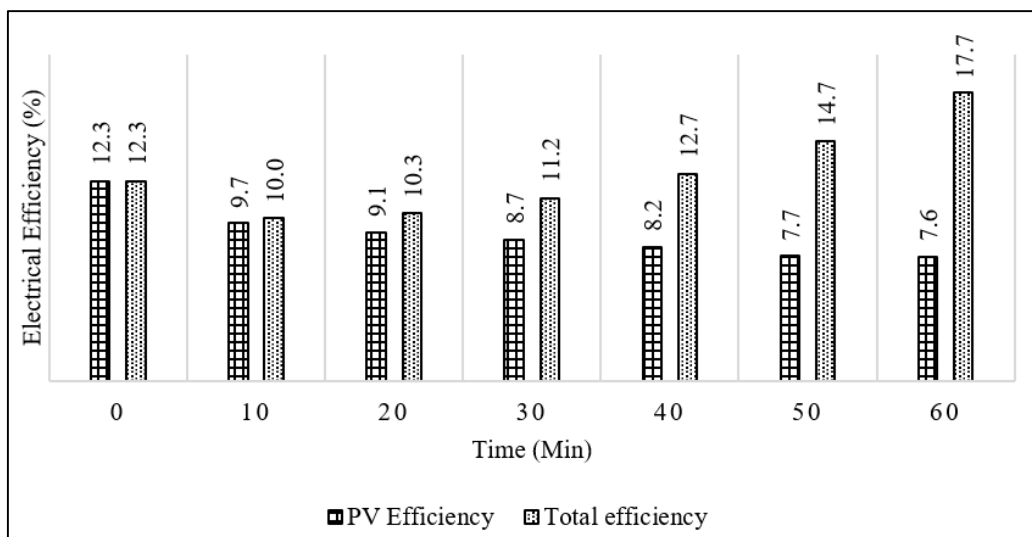
Figure 15. Electrical efficiency of the system.

As previously mentioned in Figure 10, the proposed system has managed to cool down the PV panel by 22.6°C, which gives an electrical improvement of 2.7% compared to PV panel alone. Therefore, the proposed system has a total of 12.8% improvement compared to the standard PV panel setup.

4. Conclusion

Using a passive cooling system with multiple layers helps to cool the PV panel down without any additional equipment such as a heat pipe or fan which will help to minimize the efficiency drop from the additional cooling components. From Table 4, it can be seen that the temperature of the PV panel with multiple layers is approximately 23°C cooler compared to the PV panel alone. This is due to increasing the thermal conductivity of the system by adding multiple layers whereas for PV panel alone, heat can only escape through air. From Figure 15, it can be seen that as time increases, the efficiency of the PV panel decreases. The final temperature of the PV panel was approximately 66.6°C, and the initial temperature was approximately 27°C, which shows a temperature increase of 39.6°C. This shows that the efficiency of the PV panel drops approximately 0.1% for every 1°C increment. In contrast, the electrical efficiency of the PVT-TEG system increases as time increases, proving that the excess heat from the PV panel is converted to electricity with the help of the TEG. The PCM helps to store the heat from the PV panel and redistribute it for thermoelectric conversion while at the same time helping to lower the operating temperature of PV panel. After 1 hour of heating, it can be seen that the electrical efficiency of the PVT-TEG system is 17.7%, an additional of 2.7% improvement due to heat extraction. This gives an improvement of 12.8% compared to PV panel alone.

References

1   P. Moraitis, R. E. I. Schropp, and W. G. J. H. M. van Sark, "Nanoparticles for Luminescent Solar Concentrators - A review," *Opt. Mater. (Amst).*, vol. 84, pp. 636–645, 2018, doi: https://doi.org/10.1016/j.optmat.2018.07.034.

2   Y. Andrea, T. Pogrebnaya, and B. Kichonge, "Effect of Industrial Dust Deposition on Photovoltaic Module Performance: Experimental Measurements in the Tropical Region," *Int. J. Photoenergy*, vol. 2019, p. 1892148, 2019, doi: 10.1155/2019/1892148.

3   Y. Tian and C. Y. Zhao, "A review of solar collectors and thermal energy storage in solar thermal applications," *Appl. Energy*, vol. 104, pp. 538–553, 2013, doi: 10.1016/j.apenergy.2012.11.051.

4   A. Ibrahim, M. Y. Othman, M. H. Ruslan, S. Mat, and K. Sopian, "Recent advances in flat plate photovoltaic/thermal (PV/T) solar collectors," *Renew. Sustain. Energy Rev.*, vol. 15, no. 1, pp. 352–365, 2011, doi: 10.1016/j.rser.2010.09.024.

5   C. Lamnatou and D. Chemisana, "Photovoltaic/thermal (PVT) systems: A review with emphasis on environmental issues," *Renew. Energy*, vol. 105, pp. 270–287, 2017, doi: 10.1016/j.renene.2016.12.009.

6   A. G. Lupu, V. M. Homutescu, D. T. Balanescu, and A. Popescu, "A review of solar photovoltaic systems cooling technologies," *IOP Conf. Ser. Mater. Sci. Eng.*, vol. 444, no. 8, 2018, doi: 10.1088/1757-899X/444/8/082016.

7   S. Shittu, G. Li, Q. Xuan, X. Zhao, X. Ma, and Y. Cui, "Electrical and mechanical analysis of a segmented solar thermoelectric generator under non-uniform heat flux," *Energy*, vol. 199, p. 117433, 2020, doi: 10.1016/j.energy.2020.117433.

8   Y.-Y. Wu, S.-Y. Wu, and L. Xiao, "Performance analysis of photovoltaic–thermoelectric hybrid system with and without glass cover," *Energy Convers. Manag.*, vol. 93, pp. 151–159, 2015, doi: https://doi.org/10.1016/j.enconman.2015.01.013.

9   B. Kılkış, "Development of a composite PVT panel with PCM embodiment, TEG modules, flat-plate solar collector, and thermally pulsing heat pipes," *Sol. Energy*, vol. 200, no. October, pp. 89–107, 2020, doi: 10.1016/j.solener.2019.10.075.

10   F. Rajaee, M. A. V. Rad, A. Kasaeian, O. Mahian, and W. M. Yan, "Experimental analysis of a photovoltaic/thermoelectric generator using cobalt oxide nanofluid and phase change material heat sink," *Energy Convers. Manag.*, vol. 212, no. February, p. 112780, 2020, doi: 10.1016/j.enconman.2020.112780.

11   A. Kolahan, S. R. Maadi, A. Kazemian, C. Schenone, and T. Ma, "Semi-3D transient simulation of a

nanofluid-base photovoltaic thermal system integrated with a thermoelectric generator," *Energy Convers. Manag.*, vol. 220, no. May, p. 113073, 2020, doi: 10.1016/j.enconman.2020.113073.

12   S. Soltani, A. Kasaeian, A. Lavajoo, R. Loni, G. Najafi, and O. Mahian, "Exergetic and enviromental assessment of a photovoltaic thermal-thermoelectric system using nanofluids: Indoor experimental tests," *Energy Convers. Manag.*, vol. 218, no. April, 2020, doi: 10.1016/j.enconman.2020.112907.

13   J. Zhang, H. Zhai, Z. Wu, Y. Wang, H. Xie, and M. Zhang, "Enhanced performance of photovoltaic–thermoelectric coupling devices with thermal interface materials," *Energy Reports*, vol. 6, pp. 116–122, 2020, doi: 10.1016/j.egyr.2019.12.001.

14   A. Makki, S. Omer, Y. Su, and H. Sabir, "Numerical investigation of heat pipe-based photovoltaic-thermoelectric generator (HP-PV/TEG) hybrid system," *Energy Convers. Manag.*, vol. 112, pp. 274–287, 2016, doi: 10.1016/j.enconman.2015.12.069.

15   R. Bjørk and K. K. Nielsen, "The performance of a combined solar photovoltaic (PV) and thermoelectric generator (TEG) system," *Sol. Energy*, vol. 120, pp. 187–194, 2015, doi: 10.1016/j.solener.2015.07.035.

16   B. S. Dallan, J. Schumann, and F. J. Lesage, "Performance evaluation of a photoelectric-thermoelectric cogeneration hybrid system," *Sol. Energy*, vol. 118, pp. 276–285, 2015, doi: 10.1016/j.solener.2015.05.034.

17   C. Babu and P. Ponnambalam, "The theoretical performance evaluation of hybrid PV-TEG system," *Energy Convers. Manag.*, vol. 173, pp. 450–460, 2018, doi: https://doi.org/10.1016/j.enconman.2018.07.104.

18   J. Darkwa, J. Calautit, D. Du, and G. Kokogianakis, "A numerical and experimental analysis of an integrated TEG-PCM power enhancement system for photovoltaic cells," *Appl. Energy*, vol. 248, pp. 688–701, 2019, doi: https://doi.org/10.1016/j.apenergy.2019.04.147.

19   G. Li, S. Shittu, K. zhou, X. Zhao, and X. Ma, "Preliminary experiment on a novel photovoltaic-thermoelectric system in summer," *Energy*, vol. 188, p. 116041, 2019, doi: 10.1016/j.energy.2019.116041.

20   J. Zhang and Y. Xuan, "An integrated design of the photovoltaic-thermoelectric hybrid system," *Sol. Energy*, vol. 177, no. November 2018, pp. 293–298, 2019, doi: 10.1016/j.solener.2018.11.012.

21   A. A. Kadhem, N. I. A. Wahab, and A. N. Abdalla, "Wind energy generation assessment at specific sites in a Peninsula in Malaysia based on reliability indices," *Processes*, vol. 7, no. 7, 2019, doi: 10.3390/pr7070399.

22   H. Li, L. Rong, C. Zong, and G. Zhang, "A numerical study on forced convective heat transfer of a chicken (model) in horizontal airflow," *Biosyst. Eng.*, vol. 150, pp. 151–159, 2016, doi: https://doi.org/10.1016/j.biosystemseng.2016.08.005.